Spectral monitoring of moorland plant phenology to identify a temporal window for hyperspectral remote sensing of peatland

Beth Cole [a,b,*], Julia McMorrow [a], Martin Evans [a]

[a] Upland Environments Research Unit, School of Environment and Development, University of Manchester, Oxford Road, Manchester M13 9PL, UK
[b] Centre for Landscape and Climate Research (CLCR), University of Leicester, University Road, Leicester LE1 7RH, UK

ABSTRACT

Recognising the importance of the timing of image acquisition on the spectral response in remote sensing of vegetated ecosystems is essential. This study used full wavelength, 350–2500 nm, field spectroscopy to establish a spectral library of phenological change for key moorland species, and to investigate suitable temporal windows for monitoring upland peatland systems. Spectral responses over two consecutive growing seasons were recorded at single species plots for key moorland species and species sown to restore eroding peat. This was related to phenological change using narrowband vegetation indices (Red Edge Position, Photochemical Reflectance Index, Plant Senescence Reflection Index and Cellulose Absorption Index); that capture green-up and senescence related changes in absorption features in the visible to near infrared and the shortwave infrared. The selection of indices was confirmed by identifying the regions of maximum variation in the captured reflectance across the full spectrum. The indices show change in the degree of variation between species occurring from April to September, measured for plant functional types. A discriminant function analysis between indices and plant functional types determines how well each index was able to differentiate between the plant functional groups for each month. It identifies April and July as the two months where the species are most separable. What is presented here is not one single recommendation for the optimal temporal window for operational monitoring, but a fuller understanding of how the spectral response changes with the phenological cycle, including recommendations for what indices are important throughout the year.

© 2014 International Society for Photogrammetry and Remote Sensing, Inc. (ISPRS) Published by Elsevier B.V. Open access under CC BY license.

1. Introduction

To understand the optimal timing for image acquisition of hyperspectral images of vegetation, detailed information is required about the spectral characteristics of natural species over the growing season. Comparison of vegetation spectral behaviour needs an understanding of the seasonal as well as environmental characteristics for the ecosystem of interest. Interpretation of spectral data in relation to vegetation is dependent upon the temporal window in which it was collected. An understanding of the variations in spectral response throughout the phenological cycle is imperative to be able to interpret remotely sensed data successfully. The timing of image acquisition is important in vegetation studies. Knowledge of spectral responses to phenological change informs optimum acquisition windows for the purpose of the study whilst knowing the spectral response of the vegetation at the time of image acquisition helps define the best methods of analysis.

The use of multi-temporal data is established for global and large scale land cover classifications. However, to maximise the impact of multi and hyper-temporal analysis there is still a need to understand the seasonal spectral response of vegetation. Inter-seasonal spectral variation is limiting the accuracy of classification techniques, and to refine these a better understanding of seasonal spectral variation is needed (Hesketh and Sánchez-Azofeifa, 2012). Imaging spectroscopy analysis of seasonal changes in vegetation have been limited (Dennison and Roberts, 2003). Miller et al. (1991) identify the gap in knowledge of seasonal and short term variations of vegetation red-edge reflectance characteristics for forest areas. Recent investigations into the leaf-level spectro-temporal variability (Hesketh and Sánchez-Azofeifa, 2012), are addressing this gap in tropical forests, however there is still a limited amount of research at this fine scale. There has

been a number of recent studies using the phenological differences among plant species to map invasive species, in rainforests (Somers and Asner, 2012, 2013), temperate forests (Burkholder et al., 2011) and riparian areas (Fernandes et al., 2013). This application requires identification of vegetation at a species level and so optimizing the spectral separability of the species through intensive monitoring of species dynamics is essential to determine the time to discriminate between species.

Peatlands provide vital ecosystem services, including carbon storage, biodiversity, water supply and agricultural uses (Bonn et al., 2009; Holden et al., 2007; Van der Wal et al., 2011). The importance of peatlands is becoming widely recognised as a result in increased awareness of their potential to sequester and store carbon (Worrall et al., 2007), which is only possible when they are in a favourable condition with a vegetation cover to reduce erosion (Bellamy et al., 2005). Blanket bogs are a UK Biodiversity Action Plan (BAP) priority habitat, so peatland restoration is a tool that addresses UK government public service agreement targets for biodiversity, and soil and water protection in uplands. Remote sensing has the potential to provide tools for habitat monitoring and surveillance of many European Commission (EC) directive Annex 1 habitats and BAP priority habitats (Medcalf et al., 2011). Remote sensing of peatlands offers the potential to monitor restoration success by charting the succession of vegetation communities. However spectral differences between plant communities are subtle and change seasonally (Milton et al., 2005). Ecologically, they consist of a wide diversity and complexity in the composition and interaction of different vegetation types (Mehner et al., 2004).

Early work on moorland remote sensing (Morton, 1986) showed that a greater understanding of the phenological change in dominant moorland species was needed. Work on the spectral properties of a single species have improved this understanding (Harris, 2008; Mac Arthur and Malthus, 2008); however, there is still a need to develop a spectral library of key moorland species and their phenological change to enable the monitoring of ecosystem function, and vegetation succession, in the heterogeneous communities of peatlands (Schaepman-Strub et al., 2008).

This article addresses the knowledge gap of spectral-temporal response of upland vegetation over the seasonal cycle based on a field spectroscopy monitoring experiment of single species plots throughout spring autumn of 2009 and 2010. The analysis evaluates established narrow-waveband indices in identifying phenological change and the point in the season when plant functional groups are spectrally most distinguishable. Finally, recommendations for the optimal time for operational monitoring are discussed.

2. Changes in biophysical properties of vegetation over the phenological cycle

The spectral reflectance of vegetation is determined by the leaf surface properties, internal structure, and the concentrations and distributions of leaf biochemical components (Penuelas and Filella, 1998). Variations in the canopy structure are the dominant control on canopy reflectance data, however the relative contributions of tissue and structural attributes vary by wavelength, both between and within vegetation types (Asner, 1998). Changes in plant physiological properties are indicators of processes occurring within the leaf and canopy stand of vegetation. Leaf pigment concentrations are symptomatic of these changes and can be characterised by measuring the spectral reflectance of vegetation in a rapid, and importantly, non-destructive manner at a range of spatial scales.

Numerous spectral indices have been developed to estimate leaf pigment content. A subset of established narrow waveband indices that monitor the concentrations of chlorophyll and carotenoids have been selected in this study as indicators of senescence, which can be related to phenology. During senescence, chlorophylls de-

grade faster than carotenes so carotenoids pigments are unmasked and subsequently become the dominant chemical in the leaves (Elvidge, 1990; Kumar et al., 2001).

Chlorophyll-a and -b are the essential pigments in photosynthesis that convert light energy into stored chemical energy. Chlorophyll concentrations decrease during plant senescence (Fang et al., 1998), therefore changes in chlorophylls in the plant are indicative of phenological state as well as stress and stage of development (Blackburn, 2006; Gitelson and Merzlyak, 1997). Carotenoids are composed of carotenes and xanthophylls. Along with chlorophylls, carotenes absorb incident radiation and contribute to photosynthesis. The epoxidation state (EPS), expressing the relative concentrations of the different xanthophyll cycle pigments, is a useful indicator of changes in photosynthetic activity (Gamon et al., 1992).

Alongside this, changes in reflectance of the non-pigment biochemical leaf components at wavelengths above 700 nm also characterise vegetation senescence and phenological conditions. Biochemical attributes such as water, nitrogen, cellulose and lignin have measureable absorption and scattering features at these longer wavelengths (Kokaly et al., 2009). Strong water absorptions in particular characterise the SWIR region, above 1300 nm. Leaf water content therefore dominate the reflectance in this region (Kumar et al., 2001). During senescence, most compounds such as nitrogen, glucose and starch are withdrawn by the plant and the bulk of the remaining material is its cellular constituents such as cellulose-lignin (Elvidge, 1990). Cellulose and lignin are both structural components of leaf cell walls. Although they are different chemical components, they are complexly intertwined and their spectral absorbance features overlap (Kokaly et al., 2009). It is therefore common to combine the two together as cellulose-lignin or ligno-cellulose (Daughtry et al., 2004).

Traditional remote sensing of vegetation uses indices based on broad band sensors such as the Normalized Difference Vegetation Index (NDVI). Detailed physiological changes and processes that occur on smaller spectral scales are not captured with this approach (Blackburn, 2006; Gamon et al., 1992, 2001; Garbulsky et al., 2011; Penuelas et al., 1995; Stylinski et al., 2002; Vogelmann et al., 1993). Saturation of NDVI occurs at relatively low values of chlorophyll-a (Gitelson and Merzlyak, 1994), proving it unsuitable for distinguishing between very green leaves. We therefore look to narrow band indices to improve our ability to monitor vegetation function and differences between species, by enhancing the spectral features of the biophysical properties undergoing change during plant senescence.

There are few published papers relating foliar pigment indices to upland species. They have mainly been applied to a few and relatively simple species such as crops (Gamon et al., 2001; Inoue and Penuelas, 2006; Sims and Gamon, 2002) and forests (Filella et al., 2009; Sims and Gamon, 2002). Work by Nichol and Grace (2010) investigated the application of chlorophyll and carotenoid indices to *Calluna vulgaris*. Their work highlights the problems of applying universal indices to a structurally and biochemically complex species and showed the knowledge gap in applying these indices to ecologically important species. Correlations have been shown between the water content of Sphagnum mosses, a key indicator species in upland peatlands, and PRI (Harris, 2008; Van Gaalen et al., 2007), but there is still a gap in the application to these ecologically important environments.

3. Method

3.1. Study site and species

The spectral measurements were made on Blackhill, an upland blanket peatland undergoing restoration, in the Peak District National Park (PDNP) in the southern Pennines, in Northern England (Fig. 1). The peatlands of the PDNP, are a fragile environment

situated at the south-eastern extent of the upland peatlands in the UK, and also at the southern climatic boarder of blanket bog distribution (Tallis, 1997).

The species recorded are shown in Table 1, and were selected to represent typical blanket bog peatland species. All species, with the exception of nurse grasses, are representative of the Mire Communities in the UK National Vegetation Classifications (NVC) present on this complex site. The site includes peatland in various states of disturbance, from intact to degraded blanket bog and areas undergoing restoration. The vegetation is a complex pattern of NVC M19 *Calluna vulgaris–Eriophorum vaginatum* blanket mire and the slightly more impoverished NVC M20 *Eriophorum vaginatum* blanket & raised mire, often associated with disturbances in the vegetation community. Also present is the NVC M3 *Eriophorum angustifolium* bog pool community, which is a typical of recent or disturbed bog pools or often forms an early seral stage in the transition from exposed peat back to mire vegetation (Elkington et al., 2002). The nurse grasses are graminoid species used in restoration to establish an initial cover of vegetation on the eroded peat surface. For restoration monitoring, it is important to be able to differentiate between the nurse grass crop and sedges.

3.2. Sampling design

For each species, two plots of 250 mm × 250 mm were identified by a visual survey. Larger plots would have included a mixture of species. For each plot, the specific species to be measured made up one hundred per cent of the ground cover. The plots were selected to be as close to one another as possible for logistical reasons, but also to reduce any difference in growing conditions. The study site is representative of a typical blanket bog, crucially with low slopes, likely to cause very small variability in microclimates and impacting local conditions upon the samples. More replicates would have been desirable to capture variation within species, but fewer species could have been measured in the time window available in what was a challenging environment for field radiometry, access to the site and the terrain made recording conditions difficult.

Spectral measurements were recorded between May and September in 2009 and April to August 2010. Spectral reflectance was only recorded under full solar illumination. Recordings were made on every opportunity, when illumination conditions allowed for two years; however there was approximately a 50% success rate for recording data on every attempted field visit. It was planned that measurements would be taken for every species on monthly intervals. However, due to the challenging weather conditions, recording was not at regular monthly intervals at every plot, although most species were recorded during each month.

Table 1
Species monitored.

Species	Functional group
Eriophorum vaginatum	Graminoid (Sedge)
Eriophorum angustifolium	Graminoid (Sedge)
Nurse grasses[a]	Graminoid (Grasses)
Sphagnum	Bryophyte
Polytrichum	Bryophyte
Hypnum	Bryophyte
Campylopus	Bryophyte
Calluna vulgaris	Shrub
Vaccinium myrtillus	Shrub
Empetrum nigrum	Shrub

[a] Nurse grass is a mixture of grass seeds sown as a restoration treatment. It contains *Festuca, Lolium, Agrostis,* and *Deschampsia.*

3.3. Spectral measurements

Reflectance measurements were carried out using an Analytical Spectral Device (ASD) Field Spec Pro spectrometer (Analytical Spectral Devices, Boulder, USA), collecting across the spectral range 350–2500 nm with a sampling interval of 1.4 nm and spectral resolution of 3 nm between 350 and 1000 nm, and a sampling interval of 2 nm and spectral resolution of 10–12 nm, between 1000 and 2500 nm. An 8° lens was fitted to the end of the optical fibre, giving a 100 mm field of view (FOV) from a consistent height of 720 mm from the ground surface and reducing edge effects from the plot where the canopy and species purity was less uniform.

A stable geometry is imperative for comparable data (Mac Arthur et al., 2007). A frame was used to position the ASD, enabling the same portion of the vegetation canopy to be measured at nadir three times, from each of three consistent directions, for each month over the growing season. Recording at three directions allowed for spatial variability in directional response function of the ASD (Mac Arthur et al., 2007), especially given the likely spatial variability in the position of greening and senescing canopy components within the FOV. Each measurement was averaged over 25 scans. The saved spectral file recorded contiguous spectral reflectance at an interval of 1 nm. All spectral measurements were recorded within a four hour window, two hours either side of solar noon. Using the bi-conical method of recording as defined by Milton (1987), absolute reflectance was calculated by normalizing canopy radiance by the radiance of a calibrated reflectance standard (Spectralon, Labsphere, NH, USA). A reference measurement was taken from the white panel before scanning each plot. This panel was re-calibrated (Natural Environment Research Council Field Spectroscopy Facility, NERC FSF) to account for change between field seasons.

The spectra were averaged from all readings for both plots to minimise the impact of natural variations in the recorded vegetation reflectance, for instance, variability due to individual leaf optical properties, plant structure, multiple leaves at different positions, and between plants. The results for 2009 and 2010 were averaged to reduce any effect of unusual growing conditions in one specific year. There was very little inter-annual variation in weather, and consequently phenology between the two years. Meteorological data recorded at the site between April and September, has shown 0.3 °C difference in the average temperature for the two years and an 89 mm difference in total rainfall. The sample size, and completeness of record is increased, as a result of combing the two years data.

3.4. Chlorophyll, carotenoid and cellulose indices

The selection of indices used in this analysis was determined by research in the literature for changes in spectral response believed to relate to phenological change (Table 2). This selection was confirmed by determining where in the spectrum the maximum amount of variation occurred in the response.

The red edge position, defined by the inflection point of the first derivative, was limited to the wavelength range 680–750 nm. A smoothing algorithm was first applied before calculating the first derivative curves to reduce noise. The Savitzky–Golay least-squares polynomial filter was used as defined in the Spectral Analysis and Management System (SAMS) (SAMS, 2005) with a 2nd order fitting polynomial and 5 data point interval. The other indices were calculated directly from the recorded spectra.

3.5. Discriminant function analysis

A discriminant function analysis was calculated to identify when in the phenological cycle the variation between the species is occurring. The discriminant function analysis is a multivariate

Table 2
Characteristics of narrow band vegetation indices applicable to the monitoring of plant senescence.

Index	Physical basis	Key characteristics	Key references
Red Edge Position (REP) $\lambda_{re} = \lambda_{\max} \frac{dR}{d\lambda}$	• The red edge is a relatively wide feature, so REP usually characterised by the inflection point, calculated as the maximum first derivative if high spectral resolution data is available, is used as a spectral index. • Derivatives reduce variability caused by additive constraints, such as changes in illumination, background soil or leaf surface reflectance, so is seen as more reliable over a range of leaf structures, canopy reflectance, and good for comparing between species. • REP depends on leaf chlorophyll content; therefore it is sensitive to environmental factors such as stress, drought and senescence.	• Smaller variation in REP in response to chlorophyll concentrations in green leaves and those in earlier stages of senescence. • The strong absorption feature at 670nm is easily saturated at high levels of chlorophyll-a. But later in senescence, when chlorophyll levels are very low, sharp increases are seen in this region. • 550nm and 705nm have maximum spectral sensitivity to chlorophyll content so serve as sensitive indicators for all stages of senescence.	Baranoski and Rokne (2005), Blackburn (2006), Boyer et al. (1988), Clevers and Jongschaap (2001), Curran (1989), Curran et al. (1991), Elvidge (1990), Gitelson and Merzlyak (1994, 1996), Gitelson et al. (1996), Liew et al. (2008), Penuelas and Filella (1998), Sims and Gamon (2002), Vogelmann et al. (1993)
Photochemical Reflectance Index (PRI) $(R_{531} - R_{570})/(R_{531} + R_{570})$	• Correlates with the epoxidation of xanthophyll cycle pigments and light use efficiency (LUE) of photosynthesis, and radiation use efficiency (RUE). • LUE and RUE vary significantly between species, seasons and ecosystems. • Compares reflectance in the blue region (531nm), where carotenoids and chlorophylls are absorbed, with reflectance in the red region (570nm), a chlorophyll only absorption. • Therefore, it is an index of relative carotenoids/chlorophyll ratios, referred to as bulk pigment ratios	• Changes in PRI over weeks to months reported to be a result of a change in the pool size of the carotenoids. • Changes in bulk pigment ratios (and therefore PRI), on this longer timescale can occur during senescence and can track seasonal variations in photosynthetic activity.	Filella et al. (2009), Gamon et al. (2001, 1992, 1997), Garbulsky et al. (2011), Guo and Trotter (2004), Nichol and Grace (2010), Penuelas et al. (1995), Penuelas and Filella (1998), Sims and Gamon (2002), Stylinski et al. (2002)
Plant Senescing Reflection Index (PSRI) $(R_{678} - R_{500})/R_{750}$	• Also sensitive to the chlorophyll/carotenoids ratio. • Reduction in chlorophyll during senescence increases reflectance between 550nm and 740nm, whilst retention of carotenoids produces continuing low reflectance in 400-500nm. It is this shift in the relative proportions of the pigments that captures senescence.	• Reflectance at 500nm and 670-680nm is usually highly correlated, but not when leaves which are further into senescence with low pigment concentrations and higher reflectance in the 670-680nm region. • PSRI uses the breakdown in this relationship to capture senescence induced change. • Changes in cell structure during senescence correlate to PSRI as it incorporates Visible and NIR bands. In the NIR, reflectance initially rises as scattering increases due to mesophyll breakdown, or the breakdown of cells.	Castro and Sanchez-Azofeifa (2008), Merzlyak et al. (1999)
Cellulose Absorption Index (CAI) $0.5(R_{2000} + R_{2200}) - R_{2100}$	• Makes use of SWIR to monitor water absorptions and cellulose structure. • Mean spectral reflectance in bands centred at 2000, 2100 and 2200nm are used to measure the depth of the 2100nm cellulose absorbance feature.	• Developed to monitor plant litter. • Used here as a proxy for senescent vegetation, operating via its effect on leaf moisture content. • High water content in leaves result in a wide 1900nm absorption feature whose right shoulder masks the cellulose-lignin absorption at 2100. • It is postulated here that water absorption decreases during senescence reducing the masking effect and making the cellulose absorption feature more prominent.	Curran (1989), Elvidge (1990), Nagler et al. (2000, 2003)

where R_x is the reflectance at that waveband, and λ_{re} is the wavelength position of red edge.

test of differences between groups. It allows for a difference in sample size between the data of the different months, since not all plots were revisited each time due to unfavourable weather conditions. The indices were used as predictor variables to see how well they categorised the spectral responses into the three plant functional types, graminoids, bryophytes and shrubs, used as categorical (or grouping) variables. The discriminant function analysis was run on the indices calculated for each of the individual plots, for each species, and separately for each month, thus eliminating the effects of averaging all the species and averaging both years data. Two discriminant functions were calculated (Table 3), they are weighted combinations of the four indices, similar to factors in factor analysis. The standardised discriminant function coefficients determine the degree to which each of the indices discriminates between each of the naturally occurring groups. If the groups differ, the indices are used to predict group membership. The classification determines how this compares to the original plant functional groups provided at the beginning of the analysis, and so can be seen as a measure of success for the discriminate function. The standardized coefficients compare variables measured on different scales, which is appropriate for the four indices, allowing us to see which index is having the greatest

Table 3

Results of the discriminant function analysis on the Red Edge Position (REP), Photochemical Reflectance Index (PRI), Plant Senescing Reflection Index (PSRI), and Cellulose Absorption Index (CAI), using all the variables.

		REP	PRI	PSRI	CAI
April					
Standardized canonical discriminant	1	0.43	0.10	1.11	0.59
Function coefficients	2	0.88	−1.07	0.10	0.72
Classification	95%				
May					
Standardized canonical discriminant	1	0.24	0.82	0.77	−0.70
Function coefficients	2	0.26	−0.03	0.70	0.51
Classification	68%				
June					
Standardized canonical discriminant	1	−0.11	0.78	0.20	−0.70
Function coefficients	2	0.99	0.03	1.10	−0.10
Classification	72%				
July					
Standardized canonical discriminant	1	12.38	5.76	16.8	
Function coefficients	2	1.67	−0.95	51.23	
Classification	100%				
August					
Standardized canonical discriminant	1	1.17	−0.54	1.13	0.19
Function coefficients	2	0.31	0.75	0.73	−0.48
Classification	72%				
September					
Standardized canonical discriminant	1	0.99	−0.38	1.00	0.19
Function coefficients	2	−0.45	1.21	0.49	−0.13
Classification	81%				

Fig. 1. Location map. Blackhill shown in rectangle. The Blanket Bog areas delineated by the 2012 BAP priority habitat inventory for England © Natural England copyright [2013]. Contains Ordnance Survey data © Crown copyright and database right [2013].

impact. By comparing the results for the separate discriminant function analysis for each month we can see how well the indices perform at differentiating the functional groups at different times of the phenological cycle.

The analysis was carried out twice, firstly including all the variables, or indices, together, and secondly in a stepwise approach. This allows a comparison to see which are the most important indices and if any are redundant in certain months for discrimination between the functional groups (Table 4).

4. Results and discussion

4.1. Variation across the spectral range

To determine the wavelengths exhibiting the largest changes in reflectance, the temporally-normalized reflectance for each species was calculated; as a ratio of the mean reflectance for a species for each month against the mean reflectance for that species overall months, for every wavelength. The ratio plots emphasized changes in the shape of the structure (Gamon et al., 1992). Fig. 2 summarises this information by plotting the maximum difference in the temporally-normalized reflectance between months for each species, for each wavelength. The peaks show the wavelengths that have the largest range, or display the greatest variation in absolute reflectance and can therefore be seen as the most diagnostic for phenological change on a species by species basis.

In the visible spectrum, peaks were seen in the green reflectance, 496 nm, and again in red between 670 and 682 nm, especially for the nurse grasses and *E. vaginatum*, suggesting that indices using in the visible spectrum should work well for detecting phenological change in these two species. At 760 nm, in the red edge, the next peak was seen. The chosen indices do make use of
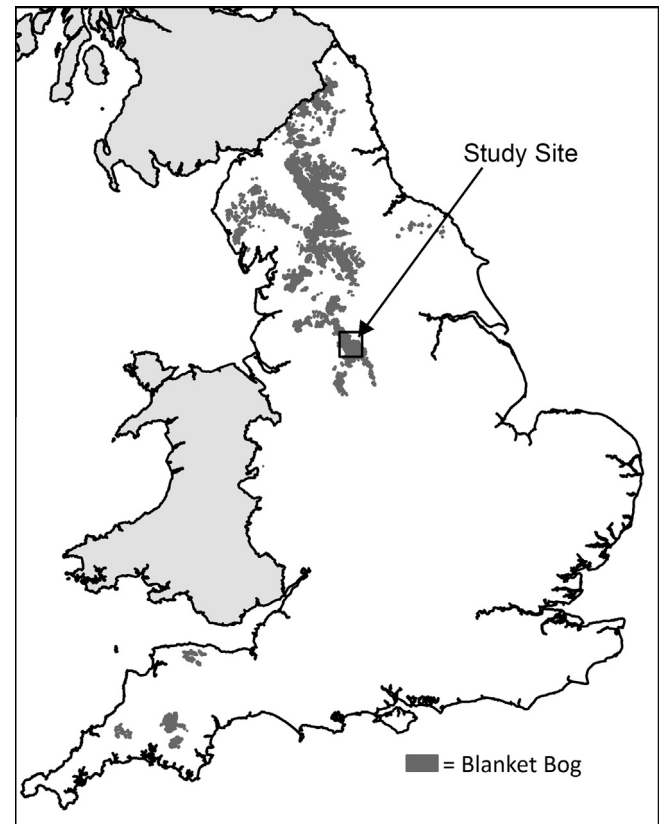
these points of increased variation, using wavelengths near to the highest points. PSRI in particular uses three wavelengths which show distinct peaks. Moving into the shortwave infrared regions, the high points appear to be either side of the main atmospheric water absorption features, at 1475 nm and 2000 nm. Strikingly, the range in the variation of reflectance increases in the longer wavelengths, as the values for the maximum increase significantly, showing the importance of the SWIR bands for this kind of diagnostic work, and the potential usefulness of CAI.

4.2. Phenological change

The measured reflectance between April and September showed a change in response to the selected indices (Fig. 3). There is a distinct difference in the REP response between the different functional groups of species. The bryophytes show very little variation, between 2 and 4 nm shift, across the whole season. In contrast, both the shrubs and the graminoid species showed a clear seasonal pattern as the plants go through the phenological cycle. The amplitude of the shift is greatest in the graminoids, with species demonstrating between a 9 and 30 nm shift, whereas the shrubs showed a range of 15 nm in *Empetrum nigrum* to 21 nm shift in *Vaccinium myrtillus*. This range of values is typical of seasonal change with REP shift often under 25 nm (Ustin et al., 2004). The pattern is shown particularly clearly by *V. myrtillus*, with a steady shift to longer wavelengths, representing a steeper slope in the red edge region as the plant leaf area increases from spring into summer, accompanied by a distinct change in colour of the leaves to bright green in June and July. The onset of senescence in August and into September showed a shift in REP

Table 4
Results of the stepwise discriminant function analysis on the Red Edge Position (REP), Photochemical Reflectance Index (PRI), Plant Senescing Reflection Index (PSRI), and Cellulose Absorption Index (CAI).

|	REP	PRI	PSRI	CAI
April				
Standardized canonical discriminant	1	0.43	1.00	
Function coefficients	2	0.93	−0.23	
Classification	81%			
May				
Standardized canonical discriminant	1	0.86	0.65	−0.69
Function coefficients	2	0.05	0.64	0.51
Classification	68%			
June				
Standardized canonical discriminant	1	0.70		−0.64
Function coefficients	2	0.72		0.78
Classification	64%			
July				
Standardized canonical discriminant	1	1.00		
Function coefficients	2			
Classification	83%			
August				
Standardized canonical discriminant	1	1.15	−0.55	1.16
Function coefficients	2	0.36	0.96	0.68
Classification	69%			
September				
Standardized canonical discriminant	1	0.78		1.13
Function coefficients	2	0.86		−0.24
Classification	81%			
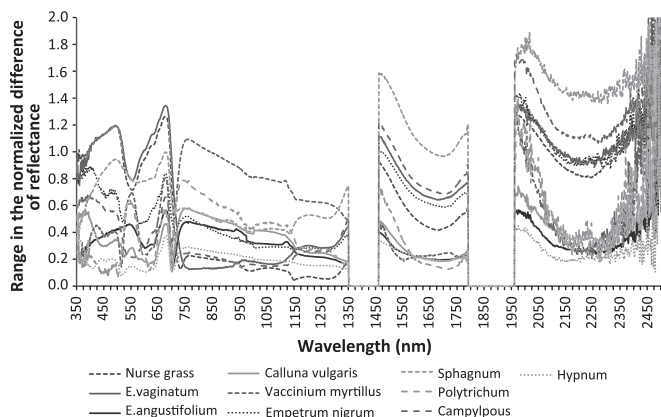
Fig. 2. The range in the temporally-normalized reflectance for each species at each wavelength. The temporally-normalized reflectance was calculated as a ratio of mean reflectance for a species for each month against the overall mean reflectance for that species. Water absorption bands were removed.

Fig. 3. Time series response of narrow band indices for each species. (a) Red Edge Position (REP). (b) Photochemical Reflectance Index (PRI). (c) Plant Senescing Reflection Index (PSRI). (d) Cellulose Absorption Index (CAI).

to shorter wavelengths. This coincides with the plant's loss of leaves in autumn, exposing the woody shoots, litter and the peat soil layers, as well as a pigment change with a reduction of chlorophyll.

The PSRI value increased during senescence due to the increase in the ratio of carotenoids to chlorophylls captured as the chlorophyll absorbance feature at 680 nm decreases (Fig. 4, *V. myrtillus*). The correlation between reflectance at 500 nm and 680 nm strengthens as the leaf area increases and the plant 'greens up' through spring into summer, then starts to decrease again through August and September.
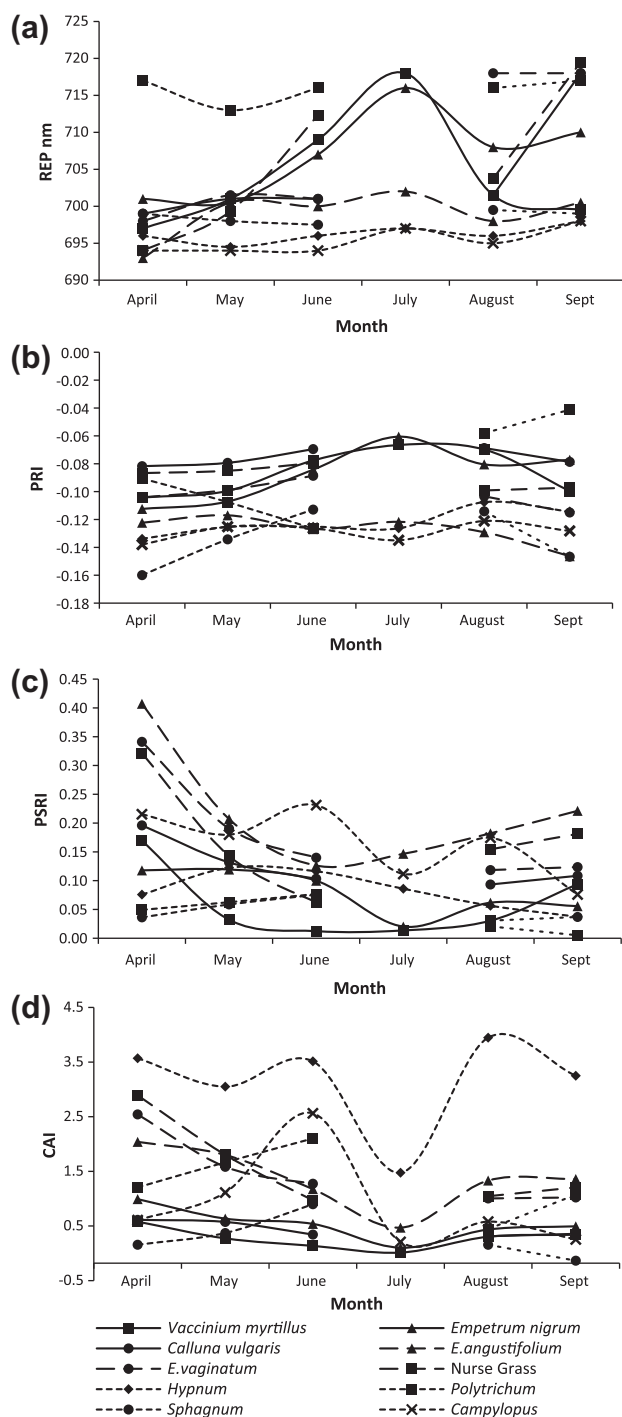
Results from previous studies show a stronger success rate for PRI than PSRI when correlating to measured chlorophyll/carotenoids ratio (Sims and Gamon, 2002; Zude, 2003). Notably, the correlation for *C. vulgaris*, for both indices was very low (Nichol and Grace, 2010). However, corresponding with the results of Castro and Sanchez-Azofeifa (2008), in both the shrubs and the graminoids the current study found that both the indices were useful to distinguish between different species, due to differences in timing of the onset of senescence.
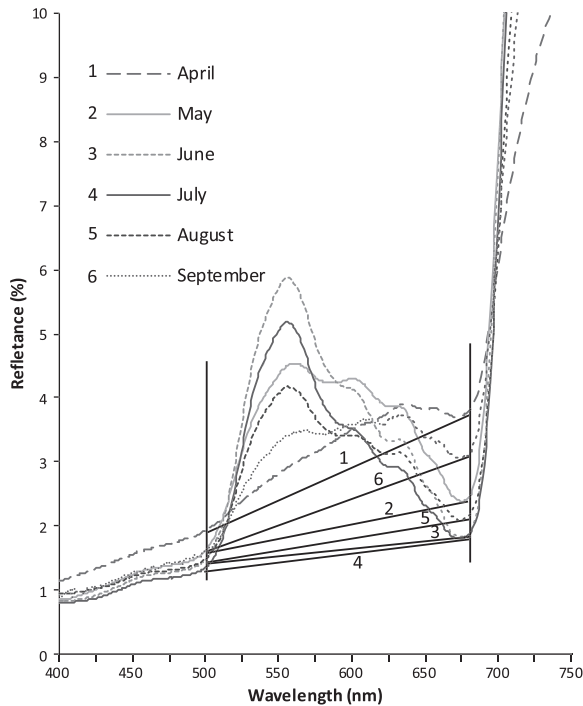
Fig. 4. Reflectance spectra of *Vaccinium myrtillus* between 400 and 750 nm from April to September. The reflectance at 500 nm and 678 nm are connected by thin lines to show the relationship between these two points, as expressed in the numerator of PSRI $(R_{678} - R_{500})/R_{750}$.

Fig. 5. Reflectance of *Eriophorum angustifolium* at 1990–2230 nm for each month over both years. The lines highlight the depth of the cellulose absorbance feature.

Fig. 6. Average Normalized Difference Water Index (NDWI), calculated as $(R_{860} - R_{1240})/(R_{860} + R_{1240})$, for each of the plant species for each month.

The PRI and PSRI indices showed an inverse relationship to one another in the phenological response of the vegetation (Fig. 3). The high PSRI values in April are present as the senescent proportion of the vegetation is still high, i.e. spring growth has not started yet. Between May and June the values dropped as the vegetation goes through its summer growth into July. Then the increase due to the start of senescence occured from August and into September. The exact timings differed between species, for example, the marked drop in *V. myrtillus* occurs between April and May, whereas *E. nigrum* falls much later between June and July. Between the functional groups, the graminoids were at their lowest PSRI value in June, but the shrubs were lowest in July. The PRI values rise steadily from April, peaking in July and then dropping back down to September. The dwarf shrubs wee the most responsive to this cycle, however the graminoid species are more separable from each other, despite showing a less strong seasonal pattern.

The importance of the senescent proportion of the vegetation canopy is demonstrated by the high CAI values in the early spring months and again by August and September. The cellulose absorbance feature becomes more pronounced as the masking effects by the foliar water are reduced, as shown in *E. angustifolium* (Fig. 4).

The deepest absorption features were seen in the early spring months before the new growth dominates, disappearing completely by July and starting to re-emerge in August and September (Fig. 5). The proportion of senescent vegetation follows the same pattern as the CAI response; high in spring, dropping into summer, and increasing through autumn. There is a hypothesised inverse relationship with water content. As foliar water content was not measured, the Normalized Difference Water Index (NDWI), a well-established broad band index sensitive to changes in liquid content of vegetation canopies (Gao, 1996), has been used as a proxy for water content. The NDWI response (Fig. 6) showed an inverse curve to CAI (Fig. 3d), reinforcing the assumption that the depth of the cellulose absorbance feature at 2100 nm is directly dictated by the masking effect of the water absorbance, as a result
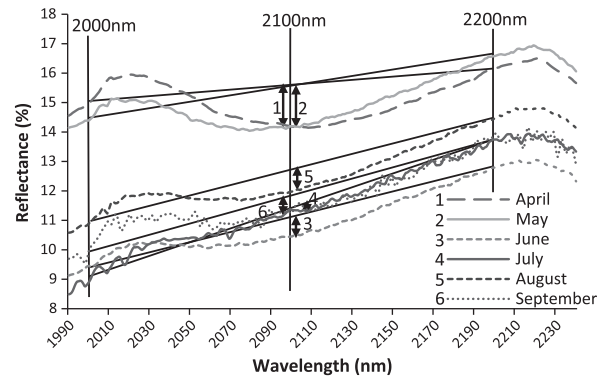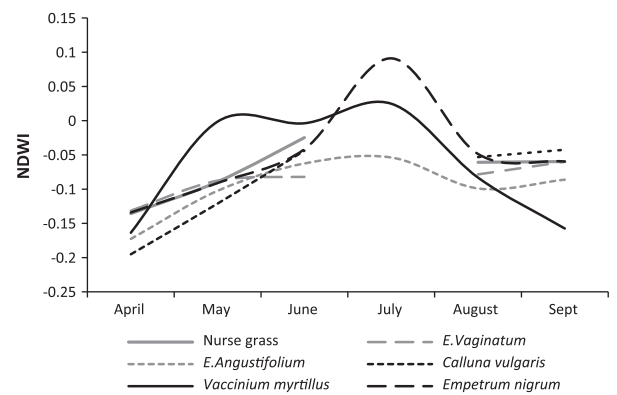
of more foliar water content in live biomass compared to senescent vegetation.

The response to CAI is similar across all species, with the lowest point in July (Fig. 3d). The bryophytes showed the same trend as the higher plants for this index, as it is not sensitive to foliar pigments and so is more applicable to mosses. The fall to low values is delayed, suggesting that the mosses take longer to accumulate their water content than the foliar species.

4.3. Interspecies variation

The narrow-band indices were used to understand when the maximum variation between species is occurring in the phenological cycle. For each index, the average monthly value was calculated for each functional group. The magnitude of difference between pairs of functional groups was plotted, (Fig. 7), showing where the most variation is, and which month best distinguishes between specific functional groups.

The REP and PRI showed a similar pattern with the maximum difference occurring firstly between the shrubs and the bryophytes and secondly between the shrubs and graminoids, peaking in July (Fig. 7a and b). There was shift in August when the onset of senescence in the graminoids occurs, making them more distinguishable from the other groups. Both PSRI and CAI, both related more to senescence, showed a slightly different response. There was a greater difference between the functional groups in April for both of these indices with a second peak in June for CAI and July for PSRI. The high level of difference in April is displaying the difference in behaviour between the functional groups throughout the winter, and the timing of new growth in the spring. Particularly with these two indices, this
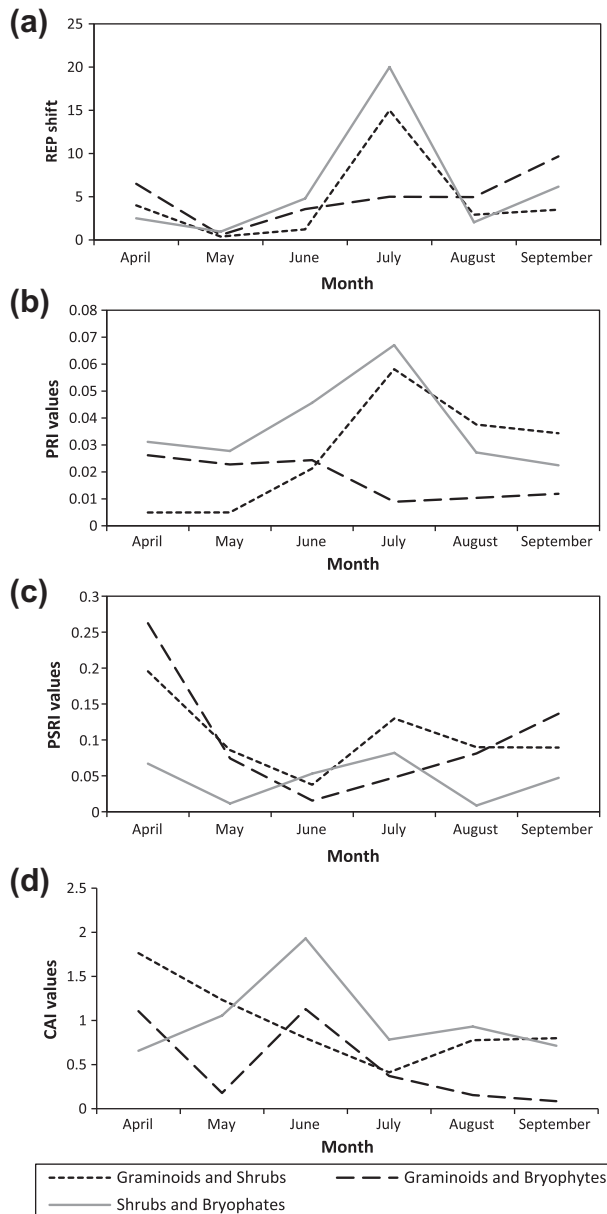
Fig. 7. Magnitude of difference in the average monthly index for pairs of functional groups. (a) Red Edge Position (REP). (b) Photochemical Reflectance Index (PRI). (c) Plant Senescing Reflection Index (PSRI). (d) Cellulose Absorption Index (CAI).

seems to be a key time for separation. Overall July is the main time of year for distinguishing between the vegetation types.

The amount of variation around the average gives a good impression of when the separation is occurring. Discriminant function analysis between the four indices and the three plant functional types confirmed these findings, that April and July are the months when the plant functional types are most separable. The larger the standardised discriminant function coefficients the greater the contribution of that variable in each discriminant function, so we can determine the degree to which each of the indices discriminates between each of groups. The classification determines how this compares to the original plant functional groups provided at the beginning of the analysis, and so the overall success at discriminating between groups.

In July the classification based on the discrimination was 100% including all the indices (Table 3); however 83% of the classification was achieved using just the PRI in the stepwise analysis (Table 4). April had a 95% classification success, with 81% ac-

counted for by PRI and PRSI. The month with the lowest classification success was May.

The index having the greatest impact in the discriminant function varied for each month. This shows that the most appropriate index for discrimination between the plant functional groups varies throughout the phenological cycle. PRI had the greatest impact through the spring to summer as the vegetation greens up and increases in leaf area, in May, June and July. PSRI had the highest impact in the spring and autumn months, in April and September, when the proportion of senescent vegetation is at its highest. REP dominated in August. Either side of this, in July and September, REP was the second most influential index, having nearly as much impact as the primary index PRI. REP therefore seems to be the most effective in discriminating in the transition from summer to autumn.

CAI seems to be under represented in the discriminant function analysis, this is surprising as the SWIR wavelengths showed the greatest amount of variation in the normalized difference reflectance for each species (Fig. 2), and the importance of the senescent vegetation has been demonstrated. It did have an influence in May and June, as shown in the stepwise analysis, and in Fig. 7 where it was the index with the greatest differentiation in averages between the shrubs and the other two functional groups.

5. Conclusion

It is the differences in reflectance indices between species at key times of the year that may have important implications for detecting species from a remote sensing perspective (Castro and San-chez-Azofeifa, 2008). The narrowband indices have shown that there is a strong, diagnostic phenological change in the spectra across a number of species.

This work sheds light onto the relative spectral-temporal response of some of the key indicator peatland species, an ecologically important ecosystem.

The vegetation was spectrally most separable in July and then in April. These two months represent very different transitional stages in the phenological cycle. In spring, the vegetation has a high proportion of senescent biomass and in July the chlorophyll pigments and the leaf area index (LAI) are at their highest. The narrow band indices are sensitive to the delay between both the onset of senescence and the beginning of the green up and also the main summer growth between species. The shifts in state of the vegetation at these times of year occur at different rates and times in the different species. The spectral separation during these two transitional phases in the phenological cycle is represented in the discrimination between functional groups using the indices.

Making recommendations for operational monitoring cannot be so simplistic. The most important variable in the discriminant function analysis varied for each month; this demonstrates that the most appropriate index to use to discriminate between the vegetation types in each month is dependent upon the ecological processes happening at that stage of the phenological cycle. Each of the indices is developed to characterise different biophysical properties in the vegetation, using different parts of the reflectance spectrum. The balance between which of these indices are most important shifts throughout the year. Understanding which part of the spectrum to focus on at different points of the season will help future monitoring. PRI is the best performing index for the spring to summer months, May–July. REP is important to capture the summer to autumn shift in July to September, and PSRI performs best in spring and autumn, when the senescent vegetation is at its highest.

The ratio of dead to live biomass seems to be very important in this ecosystem where the removal of dead litter is limited. The cellulose absorption index results showed this, as the values are high both in the spring and autumn months. The very clear seasonal

Table 5
The most influential indices for spectral separation between functional groups for each month, based upon the maximum differentiation between the average monthly index for pairs of functional groups, and the statically most important species from a discriminate function analysis.

	April	May	June	July	August	September
Graminoids and shrubs	PSRI	PSRI	PSRI	REP	PRI	PRI
	CAI	CAI	PRI	PRI	PSRI	CAI
			CAI			
Graminoids and bryophytes	REP	PRI	CAI	REP	REP	REP
	PSRI	PSRI		PRI	PSRI	PSRI
				PSRI		
				CAI		
Shrubs and bryophytes	REP	PRI	CAI	REP	CAI	CAI
	PSRI	CAI		PRI	PRI	PRI
						REP
All functional groups[a]	PRSI	PRI	PRI	PSRI	REP	PSRI
		PSRI	CAI		CAI	REP
		CAI				

[a] Statistically most important indices from discriminate function analysis.

pattern demonstrated across all the species is an indicator of the effectiveness of using the shortwave infrared reflectance to monitor how foliar structure breaks down during senescence, as well as the more established approaches looking at the pigment indices. These findings are interesting and suggest that further work could be beneficial into the complex absorption features in the SWIR, in particular the separation of the overlapping cellulose, lignin and protein absorption features at 2100 nm and 2300 nm (Kokaly et al., 2009), as the importance of the non-photosynthetic vegetation and dry matter is so important, particularly in grasslands (Asner, 1998). It is expected that continuum removal techniques (Kokaly and Clark, 1999) would prove most effective at looking at these SWIR absorption features allowing characterisation of the centre positions and shape.

In summary, the maximum spectral separation is in July and April. However the optimal time for monitoring peatland, and which index to use, is dependent upon the species prioritised. As an example, the distinction between graminoids and shrubs is easiest in July using REP and PRI, but in April using PSRI and CAI. Distinguishing between graminoids and bryophytes, however, is easiest in April using REP and PRSI, and in June using CAI. Table 5 summarises the differences in average monthly indices between the functional groups, shown in Fig. 7, providing a look up table as to the most useful indices for spectral separation at any given time.

Practical and logistical limitations to data acquisition have to be acknowledged. The data acquisition was not without difficulties, the small sample size is a limitation to the results however this was unavoidable on challenging terrain. Nevertheless, this is the only set of data there is to date, recording the multi temporal response to multiple species in this environment, so the value cannot be under estimated. The site is typical of blanket bog, and local variations in conditions will have had very minimal effects on the phenological trends observed. Although July is an important month in the separation of the species, it is also the month that in this experiment was the hardest to collect data in over both years, due to poor weather conditions on the upland site. This highlights the need to understand the effect the phenological cycle has on the spectral response of target vegetation whenever data is collected. The amount of variation in the spectral response across the season and the variation in the most appropriate index to study particular species at particular times of year demonstrated here reinforces this.

The optimum time of year for remote sensing monitoring really is dependent upon the specific interests of the application. For monitoring peatland restoration, if given the correct logistical conditions, July would be the recommended month. However, what is

provided here is not one single answer but a fuller understanding of how the spectral response changes with the phenological cycle including recommendations as to what indices are important throughout the year. Data acquisition is not always possible when desired. The analysis here identifies the best methods for any month.

The work presented here contributes new knowledge to the understanding of the detailed interactions in seasonal response of vegetation and spectral reflectance. Temporal analysis of spectral separability is important to broaden our understanding of how to translate the biochemical and structural properties of vegetation to species composition (Somers and Asner, 2012), helping refine methods for classifications that utilise multi-temporal data. The changing phenological response is critical across a range of different ecosystems, monitoring with hyper-temporal data, or determining the best time to discriminate between desired attributes will ultimately enhance the abilities of ecological remote sensing.

References

Asner, G.P., 1998. Biophysical and biochemical sources of variability in canopy reflectance. Remote Sens. Environ. 64 (3), 234–253.

Baranoski, G.V.G., Rokne, J.G., 2005. A practical approach for estimating the red edge position of plant leaf reflectance. Int. J. Remote Sens. 26 (3), 503–521.

Bellamy, P.H., Loveland, P.J., Bradley, R.I., Lark, R.M., Kirk, G.J.D., 2005. Carbon losses from all soils across England and Wales 1978–2003. Nature 437 (7056), 245–248.

Blackburn, G.A., 2006. Hyperspectral remote sensing of plant pigments. J. Exp. Bot. 58 (4), 855–867.

Bonn, A., Rebane, M., Reid, C., 2009. Ecosystem services. A new rationale for conservation of upland environments. In: Bonn, A., Allott, T., Hubacek, K., Stewart, J. (Eds.), Drivers of Change in Upland Environments. Routledge, London and New York, pp. 448–474.

Boyer, M., Miller, J., Belanger, M., Hare, E., Wu, J.Y., 1988. Senescence and spectral reflectance in leaves of Northern Pin Oak (Quercus-Palustris Muenchh). Remote Sens. Environ. 25 (1), 71–87.

Burkholder, A., Warner, T.A., Culp, M., Landenberger, R., 2011. Seasonal trends in separability of leaf reflectance spectra for *Ailanthus altissima* and four other tree species. Photogramm. Eng. Rem Sens. 77 (8), 793–804.

Castro, K.L., Sanchez-Azofeifa, G.A., 2008. Changes in spectral properties, chlorophyll content and internal mesophyll structure of senescing *Populus balsamifera* and *Populus tremuloides* leaves. Sensors 8 (1), 51–69.

Clevers, J.P.G.W., Jongschaap, R., 2001. Imaging spectrometry for agricultural applications. In: van der Meer, F.D., de Jong, S.M. (Eds.), Imaging Spectrometry: Basic Principles and Prospective Applications. Kluwer Academic Publishers, Dordrecht, pp. 157–199.

Curran, P.J., 1989. Remote-sensing of foliar chemistry. Remote Sens. Environ. 30 (3), 271–278.

Curran, P.J., Dungan, J.L., Macler, B.A., Plummer, S.E., 1991. The effect of a red leaf pigment on the relationship between red edge and chlorophyll concentration. Remote Sens. Environ. 35 (1), 69–76.

Daughtry, C.S.T., Hunt, E.R., McMurtrey, J.E., 2004. Assessing crop residue cover using shortwave infrared reflectance. Remote Sens. Environ. 90 (1), 126–134.

Dennison, P.E., Roberts, D.A., 2003. The effects of vegetation phenology on end member selection and species mapping in southern California chaparral. Remote Sens. Environ. 87 (2–3), 295–309.

Elkington, T., Dayton, N., Jackson, D.L., Strachan, I.M., 2002. National Vegetation Classification Field Guide to Mires and Heaths, JNCC.

Elvidge, C.D., 1990. Visible and near-infrared reflectance characteristics of dry plant materials. Int. J. Remote Sens. 11 (10), 1775–1795.

Fang, Z.Y., Bouwkamp, J.C., Solomos, T., 1998. Chlorophyllase activities and chlorophyll degradation during leaf senescence in non-yellowing mutant and wild type of *Phaseolus vulgaris* L. J. Exp. Bot. 49 (320), 503–510.

Fernandes, M.R., Aguiar, F.C., Silva, J.M.N., Ferreira, M.T., Pereira, J.M.C., 2013. Spectral discrimination of giant reed (*Arundo donax* L.): a seasonal study in riparian areas. ISPRS J. Photogram. Remote Sens. 80, 80–90.

Filella, I. et al., 2009. PRI assessment of long-term changes in carotenoids/chlorophyll ratio and short-term changes in de-epoxidation state of the xanthophyll cycle. Int. J. Remote Sens. 30 (17), 4443–4455.

Gamon, J.A., Penuelas, J., Field, C.B., 1992. A narrow-waveband spectral index that tracks diurnal changes in photosynthetic efficiency. Remote Sens. Environ. 41 (1), 35–44.

Gamon, J.A., Serrano, L., Surfus, J.S., 1997. The photochemical reflectance index: an optical indicator of photosynthetic radiation use efficiency across species, functional types, and nutrient levels. Oecologia 112 (4), 492–501.

Gamon, J.A., Field, C.B., Fredeen, A.L., Thayer, S., 2001. Assessing photosynthetic downregulation in sunflower stands with an optically-based model. Photosynth. Res. 67 (1–2), 113–125.

Gao, B.C., 1996. NDWI - a normalized difference water index for remote sensing of vegetation liquid water from space. Remote Sens. Environ. 58 (3), 257–266.

Garbulsky, M.F., Penuelas, J., Gamon, J., Inoue, Y., Filella, I., 2011. The photochemical reflectance index (PRI) and the remote sensing of leaf, canopy and ecosystem radiation use efficiencies a review and meta-analysis. Remote Sens. Environ. 115 (2), 281–297.

Gitelson, A., Merzlyak, M.N., 1994. Quantitative estimation of chlorophyll-A using reflectance spectra – experiments with autumn chestnut and maple leaves. J. Photochem. Photobiol. B-Biol. 22 (3), 247–252.

Gitelson, A.A., Merzlyak, M.N., 1996. Signature analysis of leaf reflectance spectra: algorithm development for remote sensing of chlorophyll. J. Plant Physiol. 148 (3–4), 494–500.

Gitelson, A.A., Merzlyak, M.N., 1997. Remote estimation of chlorophyll content in higher plant leaves. Int. J. Remote Sens. 18 (12), 2691–2697.

Gitelson, A.A., Merzlyak, M.N., Lichtenthaler, H.K., 1996. Detection of red edge position and chlorophyll content by reflectance measurements near 700 nm. J. Plant Physiol. 148 (3–4), 501–508.

Guo, J.M., Trotter, C.M., 2004. Estimating photosynthetic light-use efficiency using the photochemical reflectance index: variations among species. Funct. Plant Biol. 31 (3), 255–265.

Harris, A., 2008. Spectral reflectance and photosynthetic properties of Sphagnum mosses exposed to progressive drought. Ecohydrology 1 (1), 35–42.

Hesketh, M., Sánchez-Azofeifa, G.A., 2012. The effect of seasonal spectral variation on species classification in the Panamanian tropical forest. Remote Sens. Environ. 118, 73–82.

Holden, J. et al., 2007. Environmental change in moorland landscapes. Earth Sci. Rev. 82 (1–2), 75–100.

Inoue, Y., Penuelas, J., 2006. Relationship between light use efficiency and photochemical reflectance index in soybean leaves as affected by soil water content. Int. J. Remote Sens. 27 (22), 5109–5114.

Kokaly, R.F., Clark, R.N., 1999. Spectroscopic determination of leaf biochemistry using band-depth analysis of absorption features and stepwise multiple linear regression. Remote Sens. Environ. 67 (3), 267–287.

Kokaly, R.F., Asner, G.P., Ollinger, S.V., Martin, M.E., Wessman, C.A., 2009. Characterizing canopy biochemistry from imaging spectroscopy and its application to ecosystem studies. Remote Sens. Environ. 113, S78–S91.

Kumar, L., Schmidt, K., Dury, S.J., Skidmore, A., 2001. Imaging spectrometry and vegetation science. In: van der Meer, F.D., de Jong, S.M. (Eds.), Imaging Spectrometry: Basic Principles and Prospective Applications. Remote Sensing and Digital Image Processing. Kluwer Academic Publishers, Dordrecht, pp. 111–155.

Liew, O.W., Chong, P.C.J., Li, B.Q., Asundi, A.K., 2008. Signature optical cues: emerging technologies for monitoring plant health. Sensors 8 (5), 3205–3239.

Mac Arthur, A.A., Malthus, T.J., 2008. An object-based image analysis approach to the classification and mapping of *Calluna vulgaris* canopies. Proceedings of the Remote Sensing and Photogrammtry Society Conference 2008 'Measuring change in the Earth system'. RSPSoc, University of Exeter.

Mac Arthur, A.A., MacLellan, C., Malthus, T.J., Ieee, 2007. The implications of non-uniformity in fields-of-view of commonly used field spectroradiometers. IEEE International Geoscience and Remote Sensing Symposium (IGARSS). IEEE, Barcelona, Spain.

Medcalf, K.A., Parker, J.A., Turton, N., Finch, C., 2011. Making Earth Observation Work for UK Biodiversity Conservation – Phase 1. Project code: CR 0477. Report to the JNCC and Defra.

Mehner, H., Cutler, M., Fairbairn, D., Thompson, G., 2004. Remote sensing of upland vegetation: the potential of high spatial resolution satellite sensors. Glob. Ecol. Biogeogr. 13 (4), 359–369.

Merzlyak, M.N., Gitelson, A.A., Chivkunova, O.B., Rakitin, V.Y., 1999. Non-destructive optical detection of pigment changes during leaf senescence and fruit ripening. Physiol. Plant. 106 (1), 135–141.

Miller, J.R., Wu, J.Y., Boyer, M.G., Belanger, M., Hare, E.W., 1991. Seasonal patterns in leaf reflectance red-edge characteristics. Int. J. Remote Sens. 12 (7), 1509–1523.

Milton, E.J., 1987. Principles of field spectroscopy. Int. J. Remote Sens. 8 (12), 1807–1827.

Milton, E.J. et al., 2005. Remote Sensing of Bog Surfaces, JNCC. Report No. 366, Peterborough.

Morton, A.J., 1986. Moorland plant community recognition using Landsat MSS data. Remote Sens. Environ. 20 (3), 291–298.

Nagler, P.L., Daughtry, C.S.T., Goward, S.N., 2000. Plant litter and soil reflectance. Remote Sens. Environ. 71 (2), 207–215.

Nagler, P.L., Inoue, Y., Glenn, E.P., Russ, A.L., Daughtry, C.S.T., 2003. Cellulose absorption index (CAI) to quantify mixed soil-plant litter scenes. Remote Sens. Environ. 87 (2–3), 310–325.

Nichol, C.J., Grace, J., 2010. Determination of leaf pigment content in *Calluna vulgaris* shoots from spectral reflectance. Int. J. Remote Sens. 31 (20), 5409–5422.

Penuelas, J., Filella, I., 1998. Visible and near-infrared reflectance techniques for diagnosing plant physiological status. Trends Plant Sci. 3 (4), 151–156.

Penuelas, J., Baret, F., Filella, I., 1995. Semiempirical indexes to assess carotenoids chlorophyll-A ratio from leaf spectral reflectance. Photosynthetica 31 (2), 221–230.

Schaepman-Strub, G., Limpens, J., Menken, M., Bartholomeus, H.M., Schaepman, M.E., 2008. Towards spatial assessment of carbon sequestration in peatlands: spectroscopy based estimation of fractional cover of three plant functional types. Biogeosciences 6 (2), 275–284.

Sims, D.A., Gamon, J.A., 2002. Relationships between leaf pigment content and spectral reflectance across a wide range of species, leaf structures and developmental stages. Remote Sens. Environ. 81 (2–3), 337–354.

Somers, B., Asner, G.P., 2012. Hyperspectral time series analysis of native and invasive species in Hawaiian rainforests. Remote Sens. 4 (9), 2510–2529.

Somers, B., Asner, G.P., 2013. Invasive species mapping in Hawaiian rainforests using multi-temporal hyperion spaceborne imaging spectroscopy. IEEE J. Sel. Top. Appl. Earth Observat. Remote Sens. 6 (2), 351–359.

Stylinski, C.D., Gamon, J.A., Oechel, W.C., 2002. Seasonal patterns of reflectance indices, carotenoid pigments and photosynthesis of evergreen chaparral species. Oecologia 131 (3), 366–374.

Tallis, J.H., 1997. Peat erosion in the Pennines: the badlands of Britain. Biologist 44 (1), 277–279.

Ustin, S., Roberts, D.A., Gamon, J.A., Asner, G.P., Green, R.O., 2004. Using imaging spectroscopy to study ecosystem processes and properties. Bioscience 54 (6), 523–534.

Van der Wal, R. et al., 2011. Mountains. Moorlands and Heaths, UNEP-WCMC, Cambridge.

Van Gaalen, K.E., Flanagan, L.B., Peddle, D.R., 2007. Photosynthesis, chlorophyll fluorescence and spectral reflectance in Sphagnum moss at varying water contents. Oecologia 153 (1), 19–28.

Vogelmann, J.E., Rock, B.N., Moss, D.M., 1993. Red edge spectral measurements from sugar maple leaves. Int. J. Remote Sens. 14 (8), 1563–1575.

Worrall, F. et al., 2007. Predicting the future carbon budget of an upland peat catchment. Climatic Change 85 (1–2), 139–158.

Zude, M., 2003. Comparison of indices to predict fruit carotenoid/chlorophyll ratio non-destructively in 'Elstar' and 'Jonagold' apples. Issues Adv. Postharvest Hortic. 1 and 2 (628), 103–110.